Journal of Nano- and Electronic Physics
Vol. **14** No 5, 05001(4pp) (2022)

Журнал нано- та електронної фізики
Том **14** № 5, 05001(4cc) (2022)

Structural, Morphological and Optical Characterization of Cobalt Diselenide Grown by Direct Vapor Transport (DVT) Method

Darshan. J. Jadav*, S.M. Vyas†, A.M. Vora‡

Department of Physics, University School of Science, Gujarat University, Navarangpura, Ahmedabad – 380 009, Gujarat, India

(Received 03 August 2022; revised manuscript received 24 October 2022; published online 28 October 2022)

Enormous research and many noteworthy innovations have been done using Transition Metal Dichalcogenides (TMDCs) over the years. This class of layered semiconductor materials has found a strong foothold in the realm of device making due to theirs many versatile properties. The tunable band gap, accompanied with remarkable photonic and electronic properties, are a few of the striking features of these materials. They follow the 'MX_2' type of arrangement with van der Waals forces holding the interlayers, where M (Mo, Nb, Re, Hf etc.) symbolizes a transition metal and X (Se, S or Te, etc.) is a chalcogen atom. Among the family, cobalt is used as a dopant to perk up the properties of many compounds. The focus of the work is to grow cobalt diselenide ($CoSe_2$) by Direct Vapor Transport (DVT) method using a custom made dual-zone furnace. XRD, HRTEM-SAED, SEM-EDX and UV-VIS-NIR spectroscopy are utilized to identify their structural, morphological and optical properties. XRD and SAED results confirm the polycrystalline nature of the sample prepared; also, the results are consistent with previously reported works. SEM and HRTEM depict the surface morphology and layered structure of the prepared sample. Also, EDX confirms the stoichiometry, purity and homogeneity of the prepared sample. The direct and indirect band gaps obtained using UV-VIS-NIR spectroscopy are 3.303 eV and 3.046 eV, respectively.

Keywords: 2D materials, TMDC, Cobalt diselenide, DVT technique, HRTEM-SAED.

DOI: 10.21272/jnep.14(5).05001 PACS numbers: 78.67. – n, 81.07. – b

1. INTRODUCTION

Though graphene has been extensively researched upon the zero band gap value led to the need for investigating similar 2D materials with an appropriate energy gap [1, 2]. One of the many such discovered materials is a category of layered TMDCs [3, 4]. This class of materials exhibits an MX_2 pattern of atomic plane arrangement; with M standing for transition metal and X for chalcogen. Every individual layer has covalently bonded constituents, where weak bonds hold the multiple layers. The weaker bond across the thickness of TMDCs makes it easier to cleave the layers, hence transforming them from bulk to few-layered counterparts [5]. Commonly, a single layer of TMDC would be 0.6-0.7 nm thick, following a hexagonal structure [6-8]. However, depending upon the elemental constituents, the coordination could be octahedral or trigonal prismatic [9, 10]. In some instances, even orthorhombic or cubic structure may be followed by these materials as is reported in the case of nanocrystalline $CoSe_2$ grown by hydrothermal synthesis [11]. Though numerous methods have been testified for the synthesis of these materials; it is the quality and the desired quantity of outcome that governs the selection of growth method [7]. These layered materials have been reported to exhibit exceptional optical, mechanical and electrical properties, which under certain specific conditions can be tuned according to need [12, 13]. Band gap engineering enables to alter the electronic properties of these materials accordingly transforming them into an insulator, semiconductor or metal [14]. Their stability, non-zero band gap coupled with high mobility of carriers, make them suitable candidates for applications in semiconductor systems [15-17], lightweight wearable and flexible applications as well [18]. Tedstone et al. [19] have reported vast applications of these TMDCs, whereas Dong et al. [9] have highlighted the use of TMDCs in heterostructure fabrications.

Among TMDCs, $CoSe_2$ has been reported to be an efficient electrocatalyst for hydrogen evolution reaction [6, 20, 21], a good photocathode for water splitting experiments [10, 22] and an excellent anode for sodium-ion batteries [23, 24]. Keeping in mind the vast applications of cobalt diselenide, crystals of $CoSe_2$ were grown from its vapor phase in the present work.

2. EXPERIMENTAL

2.1 Growth and Characterization

DVT technique was preferred for the growth of $CoSe_2$ crystals to preserve the purity of the compound to be grown [25, 26]. To serve the purpose, powders of Cobalt (CDH and 99.95 % purity) and Selenium (CDH and 99.95 % purity) were taken in the desired proportion in a quartz ampoule. The ampoule containing the properly mixed powdered constituents was then introduced to a two-zone horizontal furnace. The temperature of both the zones was raised from room temperature such that the source zone and growth zone reached a temperature of 1050 °C and 950 °C, respectively. The ampoule was placed in the furnace in such a way that the powder mix would be at the higher temperature region. Such high temperature enables the powder to melt and mix well with each other. The tem-

* jadavdarshanj@gmail.com
† vyassandip479@gmail.com
‡ voraam@gmail.com

perature difference of 100 °C allows the proper chemical reaction to occur at the source zone and also facilitates the transport of the reacted vapors to the growth zone. The temperature of the furnace was maintained as such for 60 h providing sufficient time for the reaction to occur. Later, the furnace was brought back to room temperature at a rate of 200 °C per 24 h. Table 1 specifies parameters followed during the growth process. The outcome of the entire process was the charge of cobalt diselenide compound.

The obtained sample was then subjected to various characterizations. Energy Dispersive Analysis of X-rays (EDAX) (OXFORD XMX N) investigated the elemental composition and homogeneity of the samples. Scanning Electron Microscopy (SEM) assisted in the morphological analysis of the sample, (JEOL Model JSM – 6390LV) was used for the purpose. High-Resolution Transmission Electron Microscopy (HRTEM) helped in observing the layered profile of the samples, (JEOL/ JEM 2100) was used for the same. X-Ray Diffraction (Bruker AXS D8 Advance) and Selected Area Electron Diffraction (SAED) confirmed the crystallinity and structural details of the sample. All characterizations of the sample were carried out by the Cochin University, Kerala under DST-SAIF and STIC Program.

Table 1 – Parameters of growth

Source zone temp.(°C)	Growth zone temp.(°C)	Holding time (hours)	Remarks
1050	950	60	Obtained charge of $CoSe_2$

3. RESULTS AND DISCUSSION

The purity, constituent elemental analysis and stoichiometry were investigated from EDX analysis. The presence of Co and Se confirms the anticipated outcome. Elemental study of $CoSe_2$ shows a homogeneous distribution of Co and Se throughout the area selected for the mapping, as shown in Fig. 1. The weight percentage obtained from the analysis also confirmed that the prepared sample is having a proper stoichiometry, which is evident from Table 2.

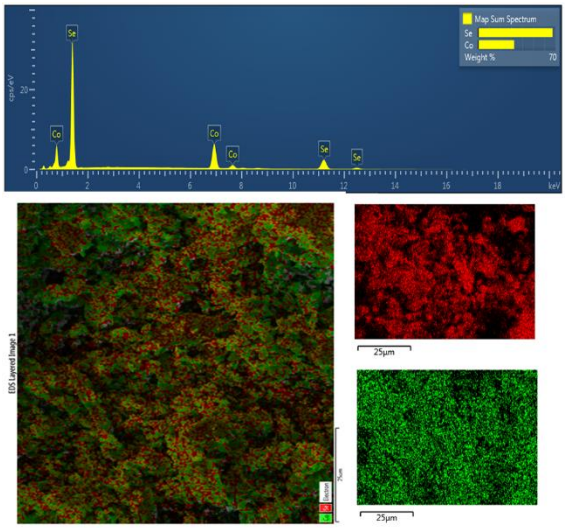

Fig. 1 – EDAX spectrum and elemental mapping of the prepared sample

The surface morphological analysis of the grown sample observed under SEM is shown in Fig. 2. Images were obtained at various magnifications; the layered growth could be observed at 1-2 µm [9, 19, 28]. Certain flat and smooth surfaces were also observed, which indicates the spreading of layers that ends where the growth terminates.

Table 2 – Weight percentage of constituent elements of $CoSe_2$ compound

Element	Weight % taken for growth	Weight % obtained from EDAX
Co	32.69	39.42
Se	67.31	60.58
Total	100	100

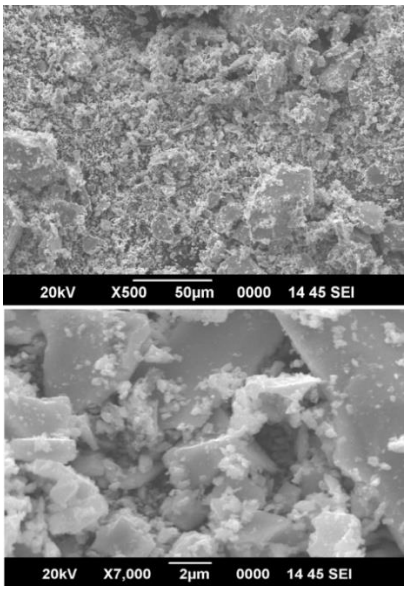

Fig. 2 – SEM images of the $CoSe_2$ charge

3.1 Powder X-Ray Diffraction (PXRD)

The powder XRD spectrum, shown in Fig. 3, assists in the structure determination of the sample. The sharpness of the XRD diffraction peaks speculates their crystallinity, while the peak position and their FWHM values help in deducing various microstructural parameters. The sharp peaks confirm that the crystals grown using the DVT method in a dual-zone furnace is crystalline. The prominent diffraction peaks are observed at (2 0 0), (2 1 0), (2 1 1), (3 1 1), (3 2 0) and (3 2 1).

The crystallite size corresponding to various peaks observed in the diffractogram has been determined by Debye-Scherrer formula. In contrast, the average crystallite size, the dislocation density and microstrain determined are tabulated in Table 3. The obtained results confirmed the polycrystalline nature of the prepared samples and were in good agreement with already reported values [9, 27].

The optical properties of $CoSe_2$ were determined from their UV-VIS-NIR spectrum shown in Fig. 4a. The absorption edge of $CoSe_2$ was around 348 nm to 362 nm. Tauc's plots (Fig. 4b, c) are constructed to evaluate the band gap values for the prepared samples [22, 27]. The value of indirect bandgap and direct bandgap was found to be 3.046 eV and 3.303 eV, respectively.

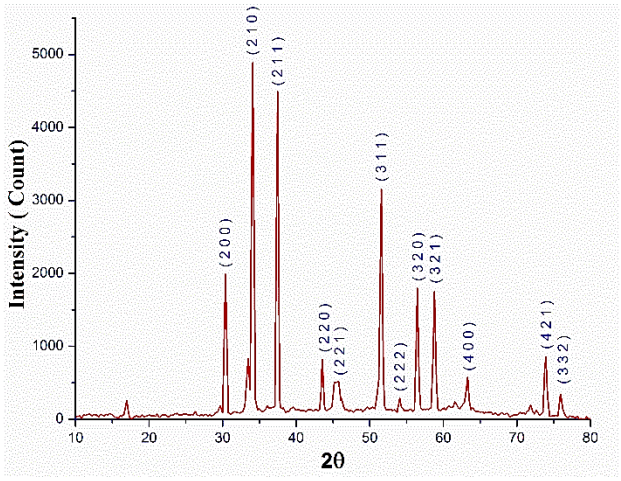

Fig. 3 – XRD pattern of $CoSe_2$ charge

Table 3 – Microstructural parameters obtained from XRD of $CoSe_2$ charge

P.n.[1]	B.a.[2]	F.M.[3]	C.S.[4]	D.D.[5]	M.S.[6]
1	30.368	0.294	27.999	1.276	4.727
2	34.078	0.301	27.605	1.312	4.285
3	37.458	0.295	28.436	1.237	3.796
4	51.565	0.326	27.063	1.365	2.945
5	56.457	0.306	29.466	1.152	2.487
6	58.797	0.313	29.133	1.178	2.424
7	73.909	0.356	27.925	1.282	2.065

[1] Peak No
[2] Braggs angle [2θ (degree)]
[3] FWHM (β)
[4] Crystallite size [D (nm)]
[5] Dislocation density [$\delta \cdot 10^{14}$ (lin m^{-4})]
[6] Microstrain [$\epsilon \cdot 10^{-4}$ (lin^{-2}m^{-4})]

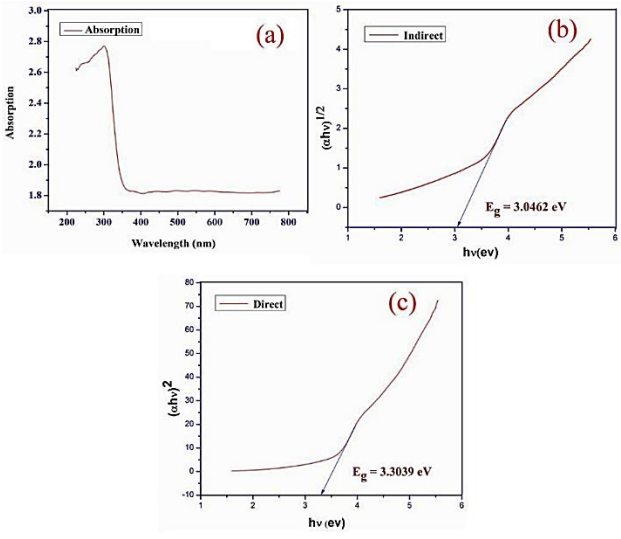

Fig. 4 – (a) Absorbance spectra, (b) Tauc's plot for indirect band gap, (c) Tauc's plot for direct band gap

The layered nature of the prepared sample was further studied using HRTEM. From Fig. 5a and Fig. 5b, nanosized flakes of the prepared material are evident. The darker region indicates a greater number of layers in comparison to the lighter region with a few layers. Fig. 5c shows the lattice fringes of the sample; the width of fringes is estimated to be around 0.21 nm, which is close to the values obtained from XRD analysis. The crystallinity of the samples was further confirmed from their SAED pattern shown in Fig. 5d. The misoriented spots and slightly diffused ring patterns in the SAED pattern clearly highlight the polycrystalline nature of the prepared sample [19, 27, 28].

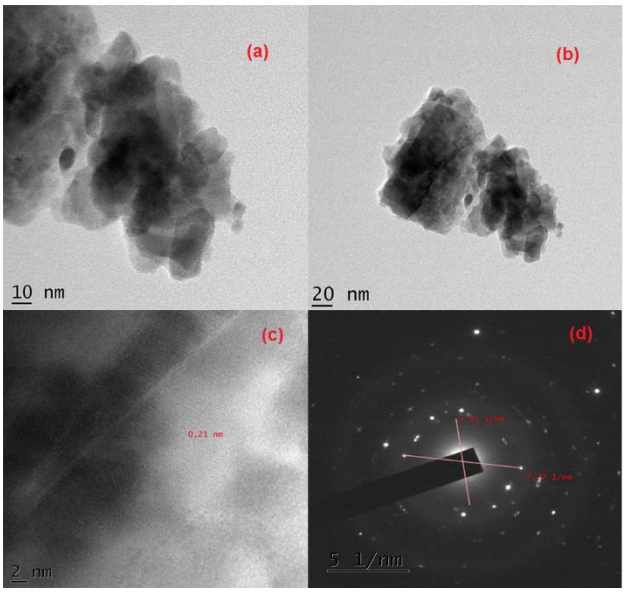

Fig. 5 – HRTEM images indicating (a, b) layered structure and nanoflakes of $CoSe_2$ charge, (c) lattice fringes of nanoflakes, (d) SAED pattern obtained from nanoflakes of $CoSe_2$ charge

4. CONCLUSIONS

$CoSe_2$ material was successfully synthesized by employing Direct Vapor Transport (DVT) method; using a custom made dual-zone furnace. Here, the EDAX analysis showed the presence of Co and Se, and the mapping showed the uniform distribution of both elements. The weight percentage of Co and Se calculated was 32.69 % and 67.31 %, respectively, which is as per the stoichiometric calculations done for $CoSe_2$. Also, the XRD analysis confirmed the polycrystalline nature with a crystal orientation at (210) plane. Several other peaks were also indexed, which were in good agreement with already reported values. While SEM and HRTEM-SAED patterns confirmed the layered nature as well as the surface morphology of the prepared sample. At a resolution of 2 nm, the lattice fringes were visible and were evaluated to be about 0.21 nm. SAED pattern also reconfirmed the crystalline nature of the prepared sample with bright spots and some slightly diffused ring pattern. UV-VIS-NIR spectroscopy analysis depicted the optical behavior of the prepared sample. Tauc's plots for both direct and indirect band gaps was done by the absorbance data obtained. The direct and indirect band gaps obtained were 3.303 eV and 3.046 eV, respectively. The value of the band gaps was following the absorbance edge obtained for the material, i.e., in the UV region of the electromagnetic spectrum.

ACKNOWLEDGEMENTS

We sincerely acknowledge the computational facility developed under DST-FIST programme from the Department of Science and Technology, Government of India, New Delhi, India and financial assistance under DRS-SAP-II from University Grants commission, New Delhi, India.

REFERENCES

1. K.S. Novoselov, V.I. Falko, L. Colombo, P.R. Gellert, M.G. Schwab, K. Kim, *Nature* **490**, 192 (2012).
2. Rui Dong, Zelei Guo, James Palmer, Yike Hu, Ming Ruan, John Hankinson, Jan Kunc, Swapan K Bhattacharya, Claire Berger, Walt A de Heer, *J. Phys. D: Appl. Phys.* **47**, 094001 (2014).
3. M. Chhowalla, H.S. Shin, G. Eda, L.-J. Li, K.P. Loh, H. Zhang, *Nat. Chem.* **5**, 263 (2013).
4. K.S. Novoselov, A. Mishchenko, A. Carvalho, A.H. Castro Neto, *Science* **353** No 6298 (2016).
5. Vijay Dixit, Salil Nair, Jolly Joy, C.U. Vyas, Alkesh B. Patel, Payal Chauhan, C.K. Sumesh, Som Narayan, P.K. Jha, G.K. Solanki, K.D. Patel, V.M. Pathak, *Eur. Phys. J. B* **92**, 118 (2019)
6. Ning Xue, Zheng Lin, Pengkun Li, Peng Diao, Qianfan Zhang, *ACS Appl. Mater. Interf.* **12** No 25, 28288 (2020).
7. F. Alex Cevallos, Shu Guo, Hoseok Heo, Giovanni Scuri, You Zhou, Jiho Sung, Takashi Taniguchi, Kenji Watanabe, Philip Kim, Hongkun Park, Robert J. Cava, ArXiv.1906.06769 (2019).
8. C.A. Patel, Kaushik R. Patel, K.D. Patel, *International Journal of Physics and Mathematical Science* **2** No 4, 17 (2012).
9. Rui Dong, Irma Kuljanishvili, *J. Vac. Sci. Technol. B* **35** No 3, 030803 (2017).
10. Y. Zhou, H. Xiao, S. Zhang, Y. Li, S. Wang, Z. Wang, C. An, J. Zhang, *Electrochimica Acta* **241**, 106 (2017).
11. Weixin Zhang, Zeheng Yang, Juewen Liu, Zehua Hui, Weichao Yu, Yitai Qian, Guien Zhou, Li Yang, *Mater. Res. Bull.* **35**, 2403 (2000).
12. X. Xu, W. Yao, D. Xiao, T.F. Heinz, *Nat. Phys.* **10**, 343 (2014).
13. Q.H. Wang, K. Kalantar-Zadeh, A. Kis, J.N. Coleman, M.S. Strano, *Nat. Nanotechnol.* **7**, 699 (2012).
14. K. Zhang, M. Park, L. Zhou, G.-H. Lee, W. Li, Y.-M. Kang, J. Chen, *Adv. Funct. Mater.* **26** No 37, 6728 (2016).
15. B. Radisavljevic, A. Radenovic, J. Brivio, V. Giacometti, A. Kis, *Nat. Nanotechnol.* **6**, 147 (2011).
16. K.F. Mak, C. Lee, J. Hone, J. Shan, T.F. Heinz, *Phys. Rev. Lett.* **105**, 136805 (2010).
17. A. Splendiani, L. Sun, Y. Zhang, T. Li, J. Kim, C.-Y. Chim, G. Galli, F. Wang, *Nano Lett.* **10**, 1271 (2010).
18. F. Schwierz, J. Pezoldt, R. Granzner, *Nanoscale* **7** No 18, 8261 (2015).
19. Aleksander A. Tedstone, David J. Lewis, Paul O'Brien, *ACS Chem. Mater.* **28**, 1965 (2016).
20. D. Kong, H. Wang, Z. Lu, Y. Cui, *J. Am. Chem. Soc.* **136** No 13, 4897 (2014).
21. W. Zhou, J. Lu, K. Zhou, L. Yang, Y. Ke, Z. Tang, S. Chen, *Nano Energy* **28**, 143 (2016).
22. Mrinmoyee Basu, Zhi-Wei Zhang, Chih-Jung Chen, Tzu-Hsiang Lu, Shu-Fen Hu, Ru-Shi Liu, *ACS Appl. Mater. Interf.* **8**, 26690 (2016).
23. K. Zhang, M. Park, L. Zhou, G.H. Lee, W. Li, Y-M. Kang, J. Chen, *Adv. Funct. Mater.* **26** No 37, 6728 (2016).
24. B. Li, Y. Liu, X. Jin, S. Jiao, G. Wang, B. Peng, G. Zhang, NANO MICRO small, V (2019).
25. Salil Nair, Jolly Joy, K.D. Patel, Pratik Pataniya, G.K. Solanki, V.M. Pathak, C.K. Sumesh, *AIP Conf. Proc.* **1961**, 030008 (2018).
26. Vijay Dixit, Salil Nair, Jolly Joy, C.U. Vyas, G.K. Solanki, K.D. Patel, V.M. Pathak, *Mater. Sci. Semicond. Proc.* **88**, 1 (2018).
27. Ruizhou Gan, Xiaohua Ma, Guorong Wang, Zhiliang Jin, *Catalysts* **9**, 616 (2019).
28. Zhiming Shi, Xinjiang Wang, Yuanhui Sun, Yawen Li, Lijun Zhang, *Semicond. Sci. Technol.* **33** No 9, 093001 (2018).

Структурні, морфологічні та оптичні характеристики диселеніду кобальту, вирощеного методом прямого переносу пари (DVT)

Darshan. J. Jadav, S.M. Vyas, A.M. Vora

Department of Physics, University School of Science, Gujarat University, Navarangpura, Ahmedabad – 380 009, Gujarat, India

Протягом багатьох років з використанням дихалькогенідів перехідних металів (TMDCs) було проведено величезну кількість досліджень та зроблено багато важливих інновацій. Цей клас шаруватих напівпровідникових матеріалів знайшов використання у сфері виготовлення пристроїв завдяки багатьом своїм універсальним властивостям. Регульована ширина забороненої зони, що супроводжується чудовими фотонними та електронними властивостями, є вражаючими особливостями цих матеріалів. Вони відповідають типу MX_2 з силами Ван-дер-Ваальса, які утримують прошарки, де M (Mo, Nb, Re, Hf тощо) символізує перехідний метал, а X (Se, S або Te тощо) є атомом халькогену. У цьому класі матеріалів кобальт використовується як добавка для покращення властивостей багатьох сполук. Метою роботи є вирощування диселеніду кобальту ($CoSe_2$) методом прямого переносу пари (DVT) за допомогою виготовленої на замовлення двозонної печі. XRD, HRTEM-SAED, SEM-EDX та UV-VIS-NIR спектроскопія використовувалися для ідентифікації структурних, морфологічних та оптичних властивостей. Результати XRD і SAED підтверджують полікристалічний характер підготовленого зразка; також результати узгоджуються з раніше повідомленими роботами. SEM та HRTEM зображують морфологію поверхні та шарувату структуру підготовленого зразка. Також EDX підтверджує стехіометрію, чистоту та однорідність підготовленого зразка. Пряма та непряма заборонені зони, отримані за допомогою UV-VIS-NIR спектроскопії, становлять 3,303 еВ та 3,046 еВ відповідно.

Ключові слова: 2D матеріали, TMDC, Диселенід кобальту, Техніка DVT, HRTEM-SAED.